7th US National Combustion Meeting of the Combustion Institute
Hosted by the Georgia Institute of Technology, Atlanta, GA
March 20-23, 2011

Mechanism reduction strategies for multicomponent gasoline surrogate fuels

K. E. Niemeyer[1] *and C. J. Sung*[2]

[1] *Department of Mechanical and Aerospace Engineering*
Case Western Reserve University, Cleveland, OH, 44106, USA
[2] *Department of Mechanical Engineering*
University of Connecticut, Storrs, CT, 06269, USA

Skeletal mechanisms for TRF mixtures were generated using DRGEPSA followed by unimportant reaction elimination. A detailed mechanism with 1389 species and 5935 reactions was reduced to different levels of complexity ranging from 386 species and 1591 reactions (lowest error) to 173 species and 689 reactions (highest error). Validation was performed using ignition delay and laminar flame speed calculations, and good agreement with the detailed mechanism was found for the error limits considered. Representative HCCI simulations of normal and low-load operation were also performed using the skeletal mechanisms. All skeletal mechanisms predict ignition to within 4 CA degrees, but only the largest skeletal mechanism to within 1 CA degree. Fuel and CO mole fraction profiles were also compared with good agreement in general, but noticeable error in the exit CO mole fraction for the very lean low-load case.

1 Introduction

The development of new internal combustion engine technology such as homogeneous charge compression ignition (HCCI) engines relies on accurate computational modeling to achieve the goals of increased efficiency and reduced emissions. In particular, chemical kinetics controls the behavior of HCCI and so simulation requires accurate description of chemistry [1]. Traditionally, gasoline is represented using a binary primary reference fuel (PRF) mixture of *n*-heptane and *iso*-octane which define 0 and 100 on the octane scale, respectively. In practice the research octane number (RON) and motor octane number (MON) are used to characterize the ON of real gasoline, and for PRF mixtures RON = MON [2]. In general, however, real gasoline has a "fuel sensitivity" defined as: $S = \text{RON} - \text{MON}$, and PRF mixtures are unable to capture this behavior. Therefore, much effort has recently been focused on developing multicomponent surrogate fuels that more accurately represent the thermochemical properties of gasoline [2–5].

As the number of components in surrogate fuels for gasoline grows, in general the size of the chemical reaction mechanism grows as well. For example, the mechanism for a three-component toluene reference fuel (TRF), containing the PRF and toluene, from Mehl et al. [5] consists of 1389 species and 5935 reactions while the mechanism for a four-component surrogate (TRF plus 1-hexene) from the same group has about 1500 species and 6000 reactions [5]. In the worst case, the computational cost of chemistry scales by the third power of the number of species when factorizing the Jacobian [6], so models of this size are far too large to include in full-scale CFD

models even without considering other complex models such as spray and turbulence. In addition, the wide range of time scales associated with the large number of species and reactions induces stiffness in the governing differential equations. Reduction of the reaction mechanisms is therefore necessary to incorporate detailed chemistry into practical simulations.

Skeletal reduction is the typical first step in a comprehensive reduction scheme, where unimportant species and reactions are removed from the detailed mechanism leaving a standard kinetic mechanism. Though many skeletal reduction methods have been demonstrated [6–8], much attention recently focused on the directed relation graph (DRG) method, developed by Lu and Law [9, 10]. Similar to the graphical representation of reaction pathways of Bendtsen et al. [11], the DRG approach maps the coupling of species onto a weighted directed graph and performs a graph search initiating at selected target species combined with an error threshold to find unimportant species for removal. Development of DRG-based skeletal reduction has since focused on variants, including DRG with error propagation (DRGEP) [12], DRG-aided sensitivity analysis [13, 14], DRGEP and sensitivity analysis (DRGEPSA) [15], and path flux analysis [16].

In the current work we present skeletal mechanisms generated using DRGEPSA followed by further unimportant reaction elimination for TRF mixtures at varying levels of detail based on the detailed mechanism of Mehl et al. [5] and apply these to representative HCCI simulations of normal and low-load (idling) operation. In doing so we seek to demonstrate that skeletal mechanisms developed with the current approach can capture the complex blending behavior of multicomponent fuel blends.

2 Methodology

2.1 Mechanism reduction

In the current work we use the DRGEPSA method of Niemeyer et al. [15], which is based on the DRGEP of Pepiot-Desjardins and Pitsch [12] followed by a sensitivity analysis of remaining species. The dependence of one species on another is modeled using a normalized contribution to the overall production or consumption rate through reactions in which both species participate. A directed graph is formed based on the direct interactions between species, where the vertices of the graph represent species and the weighted edges represent the dependence of one species on another. The overall importance of species is determined by performing a graph search initiating at user-selected target species; Dijkstra's algorithm is used for reasons discussed in detail by Niemeyer and Sung [17]. Pepiot-Desjardins and Pitsch [12] also proposed a coefficient scaling procedure to better relate the OICs from different points in the reaction system evolution that we adopt here.

In the sensitivity analysis (SA) phase, the remaining species are categorized as "limbo" or "important" species based on their DRGEP-determined importance values. Each of the limbo species are removed one-by-one to determine the error induced by their removal then sorted based on this error. The limbo species are then removed from the skeletal mechanism in order until the error reaches the user-defined limit.

We employ the same sampling method as given by Niemeyer et al. [15], where constant volume autoignition simulations are performed using SENKIN [18] with CHEMKIN-III [19]. Species are considered unimportant and removed if their overall importance value falls below a cutoff threshold $\varepsilon_{\mathrm{EP}}$, which is selected using an iterative procedure based on a user-defined error limit for ignition delay prediction [15]. Reactions are eliminated when any participating species are removed. Follow-

Error limit		# Species	# Reactions	Max. error
Comprehensive	10%	386	1591	9.2%
	20%	293	1156	19.8%
	30%	276	936	24.3%
High-temp.	10%	199	1011	9.9%
	20%	173	752	18.4%
	30%	173	689	23.1%

Table 1: Skeletal mechanisms at multiple levels of complexity generated from the detailed mechanism for ternary TRF mixtures of Mehl et al. [5] using DRGEPSA followed by unimportant reaction elimination.

ing the application of DRGEPSA, further unimportant reactions are eliminated using the method of Lu and Law [14], an approach based on the CSP importance index [20]. A reaction is considered unimportant if its importance is less than a threshold $\varepsilon_{\text{reac}}$, which is determined iteratively using the user-defined error limit.

2.2 Computational methods

Autoignition simulations are performed using SENKIN [18] with CHEMKIN-III [19]. The laminar premixed flame simulations are performed using CHEMKIN-PRO [21]. The HCCI engine simulations are performed using the Closed Internal Combustion Engine Simulator of CHEMKIN-PRO; the engine specifications are taken from Sjöberg et al. [22]: compression ratio of 14, engine speed 1200 rpm, displacement volume 981 cm^3, and connecting rod to crank radius ratio 3.2.

3 Results and discussion

3.1 Skeletal mechanisms and validation

Skeletal mechanisms at varying levels of detail are generated from a detailed mechanism for TRF (*n*-heptane, *iso*-octane, and toluene) mixtures of Mehl et al. [5], containing 1389 species and 5935 reactions, using DRGEPSA followed by further unimportant reaction elimination. Two sets of constant volume autoignition initial conditions, both covering 1–20 atm and equivalence ratios 0.5–1.5, are used to generate chemical kinetics data: 1) 700–1600 K and 2) 1000–1600 K; the former is referred to as the comprehensive range and the latter as the high-temperature range. The ternary mixture used is 60.54/20.64/18.82% (by liq. volume) toluene/*iso*-octane/*n*-heptane, or 69.1/15.4/15.6% by mole fraction, from Morgan et al. [23], which corresponds to RON = 95 and MON = 85. We refer to this mixture as TRF1. Error limits of 10%, 20%, and 30% are used and the DRGEP target species are *n*-heptane, *iso*-octane, toluene, oxygen, and the inert nitrogen (to prevent removal).

Table 1 summarizes the final results of the reduction for the comprehensive and high-temperature skeletal mechanisms, respectively. Interestingly, the 20% and 30% high-temperature skeletal mechanisms contain the same species, although the final 30% skeletal mechanism has a smaller number of reactions following unimportant reaction elimination; this is due to a large jump in error preventing the removal of any additional species. In general, however, the skeletal mechanisms consist

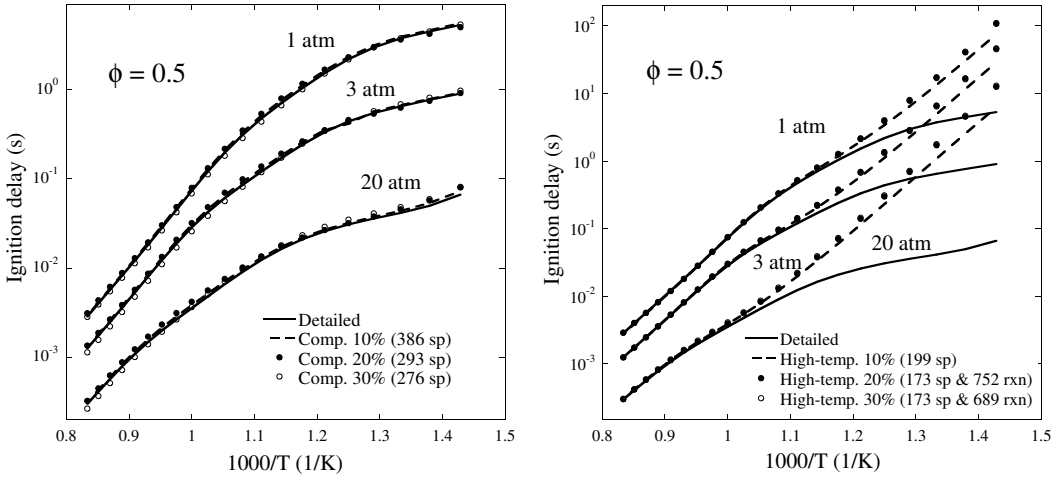

(a) Comprehensive skeletal

(b) High-temperature skeletal

Figure 1: Autoignition validation of comprehensive and high-temperature skeletal mechanisms over a range of initial temperatures and pressures and at an equivalence ratio of 0.5 using the TRF1 mixture.

of smaller number of species and reactions with increasing error limit and the high-temperature skeletal mechanisms are all more compact than the comprehensive.

Validation of the comprehensive and high-temperature skeletal mechanisms is performed with constant volume autoignition simulations over a range of initial conditions for temperature, pressure, and equivalence ratios, using the TRF1 mixture. Representative results for the comprehensive and high-temperature skeletal mechanisms are presented in Figs. 1a and Fig. 1b, respectively, using an equivalence ratio of 0.5; the stoichiometric and rich cases are omitted for brevity. All the comprehensive skeletal mechanisms well predict the results of the detailed mechanism over the full range of conditions. The high-temperature mechanisms perform well at higher temperatures as expected but fail to reproduce the low-temperature behavior. This is due to the removal of the low-temperature chemistry during the reduction procedure. Laminar flame speed calculations of the TRF1 mixture using the 10% comprehensive and high-temperature skeletal mechanisms are also performed at atmospheric pressure and with an unburned mixture temperature of 450 K. The results are are omitted here but both skeletal mechanisms show good agreement with the detailed mechanism, with the largest error less than 4%.

3.2 HCCI validation

HCCI engine simulations are also performed with each of the skeletal mechanisms at two representative conditions: 1) normal operation, with an input pressure of 1 atm and equivalence ratio of 0.5, and 2) low-load idling operation, with an inlet pressure of 1.3 atm and equivalence ratio of 0.12 [24]. In order to test the range of applicability of the skeletal mechanisms generated, a different TRF mixture is used: 69/14/17% (by liq. volume) *iso*-octane/toluene/*n*-heptane, comparable to ON87 gasoline, from Gauthier et al. [25]. The ON of this mixture is close to that used in the skeletal reduction so the ignition behavior should be similar. All skeletal mechanisms well predict ignition, with the largest error in case 1 less than 4 CA degrees and case 2 less than 2 CA

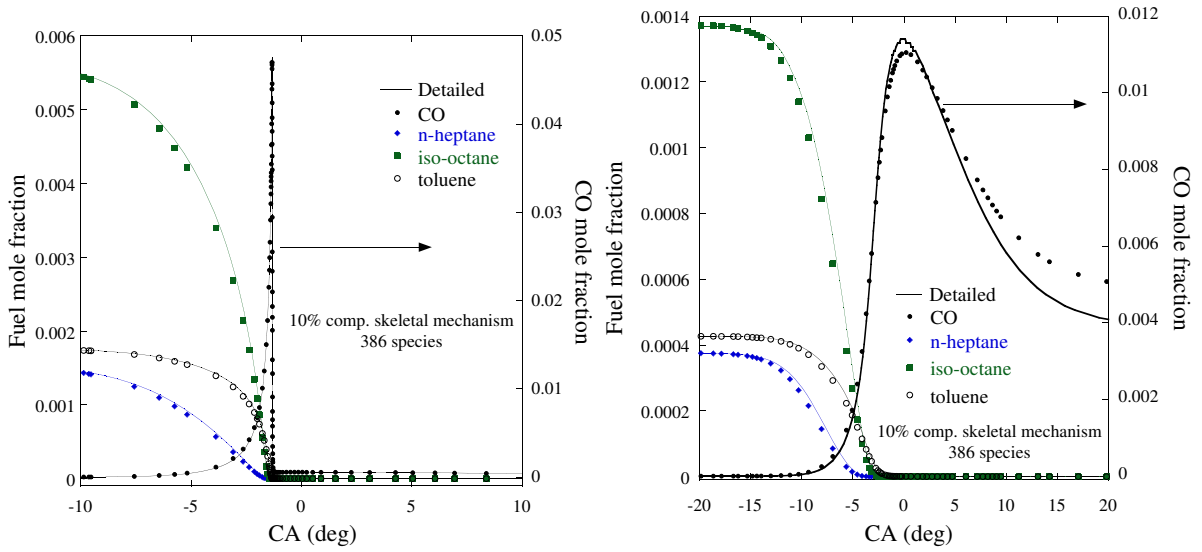

(a) Normal load

(b) Low load (idle)

Figure 2: Mole fractions of *n*-heptane, *iso*-octane, toluene, and carbon monoxide near TDC for HCCI simulations of representative normal operating and low-load (idle) conditions using the 10% comprehensive skeletal mechanisms. The skeletal mechanism results are shifted so that the point of ignition coincides with the detailed mechanism.

degrees. Only the 10% comprehensive skeletal mechanism predicts autoignition to an accuracy under 1 CA degree. Representative results using this skeletal mechanism are shown in Fig. 2; the mole fractions of the fuels and carbon monoxide are plotted against the crank angle (CA) near top dead center (TDC). In both cases the fuel breakdown is well reproduced, and the CO profile in case 1 is captured. However, noticeable error in the CO profile of case 2 is observed. While the peak CO mole fraction is accurate to ~3%, the error in exit CO mole fraction is 26% which is unacceptably large since predicting CO emissions is an important metric. It is not known whether this error is due to the extremely lean mixture of this case (outside the range of conditions used in the skeletal reduction) or the use of a different TRF mixture; further investigation is underway.

4 Conclusions

Skeletal mechanisms at varying levels of detail for a TRF mixtures are generated using DRG-EPSA followed by further unimportant reaction elimination and validated using constant volume autoignition, laminar flame propagation, and HCCI engine simulations. Some conclusions may be drawn based on the results:

- The sizes of the skeletal mechanisms, even after multiple reduction phases and with generous error limits, is still too large to be used in practical CFD simulations. Further reduction strategies and/or dynamic reduction approaches still need to be employed.

- The skeletal mechanisms demonstrated here are able to predict ignition and fuel breakdown in HCCI simulations. Tight error control (10%) is needed to capture ignition within 1 CA

degree. All the skeletal mechanisms capture the CO profile well for normal operating conditions, but noticeable error in the post-ignition CO prediction occurs at very lean (equivalence ratio 0.12) mixtures.

Acknowledgments

This work was supported by the National Science Foundation under Grant No. 0932559 and the Department of Defense through the National Defense Science and Engineering Graduate Fellowship program. The authors would also like to thank Drs. Bill Pitz and Marco Mehl of LLNL for providing the TRF detailed mechanism.

References

[1] C. K. Westbrook, Proc. Combust. Inst. 28 (2000) 1563–1577.

[2] J. C. G. Andrae, Fuel 87 (2008) 2013–2022.

[3] W. J. Pitz, N. P. Cernansky, F. Dryer, F. Egolfopoulos, J. T. Farrell, D. Friend, H. Pitsch, Development of an experimental database and chemical kinetic models for surrogate gasoline fuels, SAE 2007-01-0175, 2007.

[4] F. Battin-Leclerc, Prog. Energy Comb. Sci. 34 (2008) 440–498.

[5] M. Mehl, W. J. Pitz, C. K. Westbrook, H. J. Curran, Proc. Combust. Inst. 33 (2011) 193–200.

[6] T. Lu, C. K. Law, Prog. Energy Comb. Sci. 35 (2009) 192–215.

[7] A. S. Tomlin, T. Turányi, M. J. Pilling, Comprehensive Chemical Kinetics (1997) 293–437.

[8] M. S. Okino, M. Mavrovouniotis, Chem. Rev. 98 (1998) 391–408.

[9] T. Lu, C. K. Law, Proc. Combust. Inst. 30 (2005) 1333–1341.

[10] T. Lu, C. K. Law, Combust. Flame 146 (2006) 472–483.

[11] A. Bendtsen, P. Glarborg, K. Dam-Johansen, Comput. Chem. 25 (2001) 161–170.

[12] P. Pepiot-Desjardins, H. Pitsch, Combust. Flame 154 (2008) 67–81.

[13] X. L. Zheng, T. Lu, C. K. Law, Proc. Combust. Inst. 31 (2007) 367–375.

[14] T. Lu, C. K. Law, Combust. Flame 154 (2008) 153–163.

[15] K. E. Niemeyer, C. J. Sung, M. P. Raju, Combust. Flame 157 (2010) 1760–1770.

[16] W. Sun, Z. Chen, X. Gou, Y. Ju, Combust. Flame 157 (2010) 1298–1307.

[17] K. E. Niemeyer, C. J. Sung, Combust. Flame (2010) in press, doi:10.1016/j.combustflame.2010.12.010.

[18] A. E. Lutz, R. J. Kee, J. A. Miller, SENKIN: A FORTRAN program for predicting homogeneous gas phase chemical kinetics with sensitivity analysis, Sandia National Laboratories Report No. SAND 87-8248, 1988.

[19] R. J. Kee, F. M. Rupley, E. Meeks, J. A. Miller, CHEMKIN-III: A FORTRAN chemical kinetics package for the analysis of gas-phase chemical and plasma kinetics, Sandia National Laboratories Report No. SAND 96-8216, 1996.

[20] T. Lu, Y. Ju, C. K. Law, Combust. Flame 126 (2001) 1445–1455.

[21] Reaction Design: San Diego, CHEMKIN-PRO 15091, 2009.

[22] M. Sjöberg, J. E. Dec, W. Hwang, Thermodynamic and chemical effects of EGR and its constituents on HCCI autoignition, SAE 2007-01-0207, 2007.

[23] N. Morgan, A. Smallbone, A. Bhave, M. Kraft, R. Cracknell, G. Kalghatgi, Combust. Flame 157 (2010) 1122–1131.

[24] W. Hwang, J. E. Dec, M. Sjöberg, Fuel stratification for low-load HCCI combustion: Performance & fuel-PLIF measurements, SAE 2007-01-4130, 2007.

[25] B. M. Gauthier, D. F. Davidson, R. K. Hanson, Combust. Flame 139 (2004) 300–311.